Eur. Phys. J. D **3**, 245–256 (1998)

THE EUROPEAN PHYSICAL JOURNAL D

Spherical averaged jellium model with norm-conserving pseudopotentials

G. Mattei[a] and F. Toigo

INFM, Unità di Padova, Dipartimento di Fisica "Galileo Galilei", via Marzolo 8, I-35131, Università di Padova, Padova, Italy

Received: 3 March 1998 / Received in final form and Accepted: 2 June 1998

Abstract. The effect of non-local norm-conserving pseudo-potentials on the static and dynamic properties of Na_n and Li_n cluster with $n = 6, 8$ is investigated in the frame of self-consistent LDA calculations with spherically averaged ionic density (SAPS model). A comparison with previous calculations which use local pseudo-potentials as well with uniform averaged non-local pseudo-jellium calculation has been carried out. A better quantitative agreement with experiments has been found in the calculation of the photoresponse cross-section with respect to either simple jellium or pseudo-jellium model, even in very small clusters, where deviations from sphericity are not negligible.

PACS. 36.40.-c Atomic and molecular clusters – 71.15.Hx Pseudopotential method – 31.15.Ew Density-functional theory

1 Introduction

In the last decade a great deal of work has been devoted to the calculation of the structural and electronic properties (collective excitations, optical response, ...) of nanoclusters at different levels of sophistication. In the case of simple metal clusters the self-consistent jellium approximation in the frame of the Local Density Approximation (LDA) to Density Functional Theory (DFT) has attracted much interest due to its capability to modelize clusters even with a large number of atoms, giving a relatively good agreement with experimental data [1].

In its simplest form [2] the jellium approximation disregards the actual ionic arrangement and treats the nuclear background of the cluster as a uniformly charged sphere with a positive charge density:

$$n(\mathbf{r}) = n(r) = n_0 \Theta(R_c - r) \tag{1}$$

where $n_0 = (4/3\pi r_s^3)^{-1}$, r_s is the bulk Wigner radius, R_c is the cluster radius defined as $R_c = r_s N^{1/3}$ and N is the number of valence electrons in the cluster. Nevertheless, in order to obtain more quantitative predictions, a better treatment of the interaction between electrons and ions seems to be one effective way (another being the improvement of LDA itself) to overcome theoretical *versus* experimental discrepancies, like, for instance, the under-estimate of the red shift in the collective excitation peak (the Mie resonance) of this model. An important step in this direction has been obtained with the introduction of the spherical pseudo-jellium model [3], in which electrons and ions interact *via ab initio* norm-conserving pseudo-potentials [4]. These are designed to reproduce not only the correct valence eigenvalues but also the actual valence wave functions outside the pseudo-atom core. The main complication introduced by such potentials in the Kohn-Sham formalism is their non-locality (or better, their semi-locality, *i.e.* radial locality, but angular non-locality), whose handling increases the computational effort.

Without resorting to very time-consuming fully three-dimensional calculations to take into account the real atomic arrangement [5,6], a reasonable improvement over the simple jellium scheme can be achieved by radially averaging the atomic positions around, for instance, the center of mass of the cluster: this allows to retain the advantages of the spherical symmetry, introducing in an approximate way the geometrical arrangement of the charged nuclei, which are therefore spread over concentric shells reflecting the actual local coordination. Since the idea of spherically averaged pseudo-potentials (SAPS) model is not new [7], we wish to point out some differences between this work and previous approaches. The most important one has to do with the quality of the potentials used. We stress the fact that up to now mostly semi-empirical, local pseudo-potentials have been used in SAPS calculations [7–11]. In this work we report results obtained from *ab initio* norm-conserving pseudo-potentials, which incorporate non-local

[a] e-mail: mattei@pd.infn.it

effects connected with the core electrons. As pointed out in references [3,12], this non-locality leads to a renormalization of the electronic mass, which improves the quantitative description of the properties of such systems. Only recently the non-local effects of norm-conserving pseudopotentials in the BHS form [4] have been incorporated into the SAPS scheme. For instance, in reference [12] non-locality has been added to the SAPS model to calculate the optical response of Li clusters but with some additional approximations in the treatment of the nonlocal part of the total potential as well as in the ionic SAPS distribution. More recently, a similar approach has been followed in reference [13] for the calculation of the static properties of endohedral complex $Li_2@C_{60}$ by using the correct expression for the non-local spherical average but retaining again the simplifying restriction to the s-wave component.

Since we want to check the reliability and the limits of validity of the SAPS scheme once the full nonlocality of norm conserving pseudopotentials is included, in this work we present analytic calculations for the complete nonlocal radial average of ionic pseudopotentials, with explicit inclusion of all the angular components of the BHS pseudo-potentials and relax any further approximation beyond the SAPS prescription. Although the SAPS scheme is expected to perform better and better for large clusters, as a case study we apply this formalism to the calculation of both static and dynamic properties (optical response) of small alkali clusters and show that indeed the inclusion of p-nonlocality is significant for the smaller clusters. Moreover we show that, unexpectedly, the SAPS scheme, with nonlocality included, gives sensible results also for open shell clusters.

The paper is organized as follows: in Section 2 we analytically develop the SAPS average on the local and non-local part of the BHS pseudo-potentials in order to calculate ground-state energy and dynamic photoresponse of the clusters. In Section 3 the obtained non-local SAPS model is applied to small alkali clusters of Na and Li to test the relevance of the SAPS approximation in situation which deviate from sphericity and to compare the different contribution of non-locality in Li (for which, due to the absence of p-states in the core, the p-electrons experience the full non-locality of the ionic potential) with respect to Na (which is known to be well described already by a *local* approach [8,11]). A comparison with results obtained in the pseudo-jellium approach are reported in order to demonstrate the relevance of the ionic contribution to the photo-response cross-section.

2 The model

In the spirit of the pseudo-potential calculation we substitute atoms with *pseudo*-atoms, where only the valence electrons degrees of freedom are treated explicitly, while the inner shell electrons are frozen. The pseudo-potentials used in the present work are in the BHS form [4]:

$$\begin{aligned} v_{PS}(\mathbf{r},\mathbf{r}') &= v^{L}(\mathbf{r}) + v^{NL}(\mathbf{r},\mathbf{r}') \\ &= v_{loc}^{BHS}(r) + \sum_{lm} v_{l}^{BHS}(r)\frac{\delta(r-r')}{rr'}Y_{lm}(\hat{r})Y_{lm}^{*}(\hat{r}') \end{aligned} \quad (2)$$

where the non-local (NL) part acts on the wave functions as an integral kernel, *i.e.*:

$$v^{NL}(\mathbf{r},\mathbf{r}')\varphi_j(\mathbf{r}) \equiv \int d\mathbf{r}' v^{NL}(\mathbf{r},\mathbf{r}')\varphi_j(\mathbf{r}'). \quad (3)$$

The sum in equation (2) is usually restricted up to an l_{max} whose contribution is subtracted out becoming local so that equation (2) now reads:

$$\begin{aligned} v_{PS}(\mathbf{r},\mathbf{r}') &= v_{core}^{BHS}(r) \\ &+ \sum_{l<l_{max},m} \Delta v_{l}^{BHS}(r)\frac{\delta(r-r')}{rr'}Y_{lm}(\hat{r})Y_{lm}^{*}(\hat{r}'), \end{aligned} \quad (4)$$

with

$$v_{core}^{BHS}(r) \equiv v_{loc}^{BHS}(r) - v_{l_{max}}^{BHS}(r) \quad (5)$$

and

$$\Delta v_{l}^{BHS}(r) \equiv v_{l}^{BHS}(r) - v_{l_{max}}^{BHS}(r). \quad (6)$$

Whereas in references [12,13] the calculation is restricted to $l_{max} = 1$, we will use $l_{max} = 2$ for Na and Li, as prescribed by the BHS formulation.

Constructing first the total pseudo-atomic potential of the cluster (according to the real density $n(\mathbf{r}) = \sum_I \delta(\mathbf{r} - \mathbf{R}_I)$, $\mathbf{R}_I$ labeling the atomic sites), one has:

$$\begin{aligned} V_{tot}(\mathbf{r},\mathbf{r}') &\equiv \int d\mathbf{R}\, n(\mathbf{R})\, v_{PS}(\mathbf{r},\mathbf{r}',\mathbf{R}) \\ &= V_{tot}^{L}(\mathbf{r}) + V_{tot}^{NL}(\mathbf{r},\mathbf{r}'), \end{aligned} \quad (7)$$

where we have defined $v_{PS}(\mathbf{r},\mathbf{r}',\mathbf{R})$ as the potential of a pseudo-atom located at $\mathbf{R}$. The pseudo-jellium model [3] prescribes to fold the potential in equation (7) with the uniform jellium density of equation (1), so we can call it Uniformly Averaged Pseudo-Jellium (UAPS). One may go beyond such a simple scheme by taking into account the ionic arrangement, at least in the approximate way prescribed by the SAPS scheme. The aim is therefore to substitute the fully 3D potential with a suitably "averaged" version, which improves the basic jellium approximation either in its local formulation [2] or in the non-local one [3], while retaining its one-dimensional computational simplicity.

2.1 Ground state LDA calculation

The ground state properties of the cluster are calculated in the LDA approximation using Perdew and Zunger [14] parametrization for the exchange and correlation energy. The energy functional of the whole cluster can be written

as (Hartree atomic units are used throughout the paper):

$$E[\rho,\{\mathbf{R}_I\}] = T[\rho(\mathbf{r})] + \frac{1}{2}\int d\mathbf{r}\rho(\mathbf{r})V_H(\mathbf{r}) + \int d\mathbf{r}\rho(\mathbf{r})\varepsilon_{xc}[\rho(\mathbf{r})] + \sum_j \int d\mathbf{r}\int d\mathbf{r}'\varphi_j^*(\mathbf{r})V_{tot}(\mathbf{r},\mathbf{r}')\varphi_j(\mathbf{r}') + \frac{1}{2}\sum_{i\neq j}\frac{Z^2}{|\mathbf{R}_i-\mathbf{R}_j|} \quad (8)$$

where $V_H(\mathbf{r})$ is the Hartree potential, $\varepsilon_{xc}[\rho]$ is the exchange-correlation energy, Z is the pseudo-atomic valence and $\varphi_j(\mathbf{r})$ are the single-particles Kohn-Sham wave functions which solve:

$$\left[-\frac{1}{2}\nabla^2 + V_H(\mathbf{r}) + V_{xc}(\mathbf{r}) + V_{tot}^L(\mathbf{r})\right]\varphi_k(\mathbf{r}) + \int d\mathbf{r}' V_{tot}^{NL}(\mathbf{r},\mathbf{r}')\varphi_k(\mathbf{r}') = \varepsilon_k\varphi_k(\mathbf{r}) \quad (9)$$

where

$$V_{xc}(\mathbf{r}) \equiv \frac{\delta}{\delta\rho(\mathbf{r})}[\rho(\mathbf{r})\varepsilon_{xc}(\rho(\mathbf{r}))]. \quad (10)$$

The last term on the right hand side of equation (8) is the contribution of the point-like Coulomb interaction of the nuclei. Our main approximation is to substitute $V_{tot}(\mathbf{r},\mathbf{r}')$ with its spherical average. We do that by expanding the ionic density into spherical harmonics as follows:

$$n(\mathbf{r}) = \sum_{lm}\tilde{n}_{lm}(r)Y_{lm}(\hat{r}). \quad (11)$$

Following reference [3], we write the pseudo-potential of an ion centered at $\mathbf{R}$ as:

$$v_{PS}(\mathbf{r},\mathbf{r}',\mathbf{R}) = v_{PS}^L(\mathbf{r},\mathbf{R}) + v_{PS}^{NL}(\mathbf{r},\mathbf{r}',\mathbf{R}) \quad (12)$$

where the local part is

$$v_{PS}^L(\mathbf{r},\mathbf{R}) = \sum_{lm} Y_{lm}^*(\hat{R})Y_{lm}(\hat{r})\,\tilde{v}_{PS,lm}^L(r,R) \quad (13)$$

with

$$\tilde{v}_{PS,lm}^L(r,R) = 2\pi\int_{-1}^{1} dy\, v_{core}^{BHS}\left(\sqrt{r^2+R^2-2rRy}\right)P_l(y) \quad (14)$$

and the non-local one

$$v_{PS}^{NL}(\mathbf{r},\mathbf{r}',\mathbf{R}) = \sum_{lm,l'm',jk} Y_{lm}^*(\hat{r})Y_{l'm'}(\hat{r}')Y_{jk}(\hat{R}) \times\tilde{v}_{PS,lm,l'm',jk}^{NL}(r,r',R) \quad (15)$$

with

$$\tilde{v}_{PS,lm,l'm',jk}^{NL}(r,r',R) = \sqrt{4\pi(2j+1)}(-1)^{m'}\begin{pmatrix} l & l' & j \\ m & -m' & k\end{pmatrix}\frac{(2\pi)^2}{rr'R^2} \times\sum_\mu(-1)^\mu\begin{pmatrix} l & l' & j \\ \mu & -\mu & 0\end{pmatrix}\sum_\lambda\int_{r_<}^{r_>} dr''\Delta v_\lambda^{BHS}(r'') \times\tilde{P}_{l\mu}\left(\frac{r^2+R^2-r''^2}{2rR}\right)\tilde{P}_{\lambda\mu}\left(\frac{r^2-R^2-r''^2}{2Rr''}\right) \times\tilde{P}_{l\mu}\left(\frac{r'^2+R^2-r''^2}{2r'R}\right)\tilde{P}_{\lambda\mu}\left(\frac{r'^2-R^2-r''^2}{2Rr''}\right) \quad (16)$$

and

$$r_< = \max(|r-R|,|r'-R|) \quad r_> = \min(r+R,r'+R). \quad (17)$$

We have also defined:

$$\tilde{P}_{lm}(\cos\theta) = \sqrt{\frac{(2l+1)(l-m)!}{4\pi(l+m)!}}P_{lm}(\cos\theta) \quad (18)$$

in terms of the associated Legendre polynomials $P_{lm}(\cos\theta)$.
From equations (7, 11, 13–16) one obtains:

$$V_{tot}^L(\mathbf{r}) = \int d\mathbf{R}\sum_{lm,l'm'}\tilde{n}_{lm}(R)\,Y_{lm}(\hat{R})\,Y_{l'm'}^*(\hat{R}) \times Y_{l'm'}(\hat{r})\,\tilde{v}_{PS,l'm'}^L(r,R) = \sum_{lm}Y_{lm}(\hat{r})\left[\int_0^\infty dR\,R^2\,\tilde{n}_{lm}(R)\,\tilde{v}_{PS,lm}^L(r,R)\right] = \sum_{lm}Y_{lm}(\hat{r})\,\tilde{V}_{tot,lm}^L(r) \quad (19)$$

for the local part and

$$V_{tot}^{NL}(\mathbf{r},\mathbf{r}') = \int d\mathbf{R} \sum_{lm,l'm',l''m'',jk} \tilde{n}_{lm}(R)\, Y_{lm}(\hat{R})\, Y^*_{l'm'}(\hat{r}) \times Y_{l''m''}(\hat{r}')\, Y_{jk}(\hat{R})\, \tilde{v}^{NL}_{PS,l'm',l''m'',jk}(r,r',R) = \sum_{l'm',l''m''} Y_{l'm'}(\hat{r})\, Y^*_{l''m''}(\hat{r}') \times \sum_{lm} \int_0^\infty dR\, R^2\, \tilde{n}_{lm}(R)\, \tilde{v}^{NL}_{PS,l'm',l''m'',lm}(r,r',R) = \sum_{l'm',l''m''} Y_{l'm'}(\hat{r})\, Y^*_{l''m''}(\hat{r}')\, \tilde{V}^{NL}_{tot,l'm',l''m''}(r,r') \quad (20)$$

for the non-local part of the total ionic pseudo-potential.

As far as the local part is concerned, the SAPS scheme amounts to taking just the monopole term ($l=0, m=0$) in equation (19):

$$V_{tot}^{L}(\mathbf{r}) = Y_{00}(\hat{r})\, \tilde{V}^{L}_{tot,00}(r) + \sum_{l\neq 0,m} Y_{lm}(\hat{r})\, \tilde{V}^{L}_{tot,lm}(r) = \bar{V}^{L}_{SAPS}(r) + \Delta V^{L}_{tot}(\mathbf{r}). \quad (21)$$

This is equivalent to considering the total potential as due only to the monopole component of the ionic density:

$$n(\mathbf{r}) = n_{SAPS}(\mathbf{r}) = \tilde{n}_{00}(r) Y_{00}(\hat{r}) = \sum_I \frac{\delta(r-R_I)}{4\pi R_I^2}. \quad (22)$$

In order to use the same prescription also for the non-local part of the interaction, we single out its component arising from the monopole term of the ionic density; due to the $3j$-coefficients in equation (16), this requirement rearranges equation (20) as:

$$V_{tot}^{NL}(\mathbf{r},\mathbf{r}') = \sum_{lm} Y_{lm}(\hat{r})\, Y^*_{lm}(\hat{r}')\, \tilde{V}^{NL}_{tot,lm,lm}(r,r') + \sum_{l\neq l',m,m'} Y_{lm}(\hat{r})\, Y^*_{l'm'}(\hat{r}')\, \tilde{V}^{NL}_{tot,lm,l'm'}(r,r') = \bar{V}^{NL}_{SAPS}(\mathbf{r},\mathbf{r}') + \Delta V^{NL}_{tot}(\mathbf{r},\mathbf{r}'), \quad (23)$$

and allows to use as zero-order approximation of the complete potential $V_{tot}(\mathbf{r},\mathbf{r}')$ of equation (7) its monopole part:

$$\bar{V}_{SAPS}(\mathbf{r},\mathbf{r}') = \int d\mathbf{R}\, n_{SAPS}(\mathbf{R})\, v_{PS}(\mathbf{r},\mathbf{r}',\mathbf{R}) = \bar{V}^{L}_{SAPS}(r) + \bar{V}^{NL}_{SAPS}(\mathbf{r},\mathbf{r}'); \quad (24)$$

the remaining contributions in equations (21) and (23) may eventually be treated by perturbation theory as in reference [8]. Carrying out the SAPS scheme explicitly, from equations (19) and (20) we obtain:

$$\bar{V}^{L}_{SAPS}(r) = \frac{1}{2}\sum_I \int_{-1}^{1} dy\; v^{BHS}_{core}\left(\sqrt{r^2+R_I^2-2rR_Iy}\right), \quad (25)$$

(with $y=\cos(\widehat{\mathbf{r},\mathbf{R}_I})$) for the local part of the interaction and

$$\bar{V}^{NL}_{SAPS}(\mathbf{r},\mathbf{r}') = \sum_{lm} \bar{V}^{NL}_{l}(r,r') Y_{lm}(\hat{r}) Y^*_{lm}(\hat{r}') \quad (26)$$

with

$$\bar{V}^{NL}_{l}(r,r') \equiv \tilde{V}^{NL}_{tot,lm,lm}(r,r') = \frac{(2\pi)^2}{(2l+1)rr'} \sum_{I,\lambda,\mu} \frac{1}{R_I^2} \int_{r_<}^{r_>} dr'' \Delta v^{BHS}_{\lambda}(r'') \times \tilde{P}_{l\mu}\left(\frac{r^2+R_I^2-r''^2}{2rR_I}\right) \tilde{P}_{\lambda\mu}\left(\frac{r^2-R_I^2-r''^2}{2R_Ir''}\right) \times \tilde{P}_{l\mu}\left(\frac{r'^2+R_I^2-r''^2}{2r'R_I}\right) \tilde{P}_{\lambda\mu}\left(\frac{r'^2-R_I^2-r''^2}{2R_Ir''}\right) \quad (27)$$

for the non-local one, respectively.

Due to the required spherical symmetry of the system (implicit in Eq. (22)), one can decouple all the angular momentum components and get one-dimensional integro-differential Kohn-Sham equations for the reduced radial wave function $u_{nl}(r)$:

$$\left[-\frac{1}{2}\frac{d^2}{dr^2} + \frac{l(l+1)}{2r^2} + V_H(r) + V_{xc}(r) + \bar{V}^{L}_{SAPS}(r)\right] u_{nl}(r) + \int_0^\infty dr' \Gamma_l(r,r') u_{nl}(r') = \varepsilon_{nl} u_{nl}(r), \quad (28)$$

where

$$\Gamma_l(r,r') \equiv r\bar{V}^{NL}_{l}(r,r')r' \quad (29)$$

is the symmetric kernel due to the non-local potential. The set of equations (28) is solved self-consistently, with the Hartree and exchange-correlation potentials defined in terms of the electronic charge density:

$$\rho(r) = 2\sum_{nl} \frac{(2l+1)u^2_{nl}(r)}{4\pi r^2}\,. \quad (30)$$

2.2 TDLDA calculation

For the calculation of the dynamical properties (photo-absorption cross-section, dynamical polarizability) we use the time-dependent local density approximation (TDLDA) [15], which allows to calculate the (linear)

response of the electronic system to an external frequency-dependent potential $V_{ext}(\mathbf{r},\omega)$. This can be accomplished by the calculation of the retarded density-density correlation function obeying the following integral equation:

$$\chi(\mathbf{r},\mathbf{r}';\omega) = \chi^0(\mathbf{r},\mathbf{r}';\omega) + \int d\mathbf{r}'' \int d\mathbf{r}''' \chi^0(\mathbf{r},\mathbf{r}'';\omega) K(\mathbf{r}'',\mathbf{r}''') \chi(\mathbf{r}''',\mathbf{r}';\omega), \quad (31)$$

where the integral kernel is the residual particle-hole interaction:

$$K(\mathbf{r},\mathbf{r}') \equiv \frac{1}{|\mathbf{r}-\mathbf{r}'|} + \frac{\delta V_{xc}}{\delta\rho(r)}\delta(\mathbf{r}-\mathbf{r}'), \quad (32)$$

and $\chi^0(\mathbf{r},\mathbf{r}';\omega)$ is the correlation function calculated in the independent particle picture:

$$\chi^0(\mathbf{r},\mathbf{r}';\omega) = \sum_{i_{occ}} \varphi_i(\mathbf{r})\varphi_i^*(\mathbf{r}') \sum_j \frac{\varphi_j(\mathbf{r})\varphi_j^*(\mathbf{r}')}{\varepsilon_i+\omega-\varepsilon_j+i\delta} + \sum_{i_{occ}} \varphi_i^*(\mathbf{r})\varphi_i(\mathbf{r}') \sum_j \frac{\varphi_j^*(\mathbf{r})\varphi_j(\mathbf{r}')}{\varepsilon_i-\omega-\varepsilon_j+i\delta}. \quad (33)$$

As pointed out in reference [15], instead of computing the whole spectrum of the system required by the explicit sum over the single-particle states in equation (33), one can resort to calculation of the Green's function associated to the Schrödinger-like equation:

$$\left(-\frac{1}{2}\nabla^2 + V_{eff}(\mathbf{r}) - \varepsilon\right) G(\mathbf{r},\mathbf{r}';\varepsilon) + \int d\mathbf{r}'' V_{tot}^{NL}(\mathbf{r},\mathbf{r}'') G(\mathbf{r}'',\mathbf{r}';\varepsilon) = \delta(\mathbf{r}-\mathbf{r}') \quad (34)$$

where ε is a (complex) parameter and with

$$V_{eff}(\mathbf{r}) = V_H(\mathbf{r}) + V_{xc}(\mathbf{r}) + \bar{V}_{tot}^L(\mathbf{r}). \quad (35)$$

This procedure allows to skip the numerical-intensive explicit calculation of all the excited states (which are automatically incorporated in the calculation of the Green's function in the ground state potential, as it will be shown below), therefore restricting the attention only on those single-particle states which are occupied.

This result holds also for the integro-differential equation equation (28) as we now show: due to the real and symmetric character of the non-local interaction $V_{tot}^{NL}(\mathbf{r},\mathbf{r}')$ (as can be deduced from Eq. (27)), the single-particle eigenfunctions $\varphi_j(\mathbf{r})$'s constitutes an ortho-normal basis set:

$$\langle\varphi_j|\varphi_k\rangle = \delta_{jk}. \quad (36)$$

Therefore we may search an expansion of the Green's function in terms of this ortho-normal set $\{\varphi_j(\mathbf{r})\}$ as:

$$G(\mathbf{r},\mathbf{r}';\varepsilon) = \sum_k A_k(\mathbf{r}')\varphi_k(\mathbf{r}). \quad (37)$$

Substituting equation (37) into equation (34), one gets:

$$\sum_k A_k(\mathbf{r}') \left(-\frac{1}{2}\nabla^2 + V_{eff}(\mathbf{r}) - \varepsilon\right) \varphi_k(\mathbf{r}) + \sum_k A_k(\mathbf{r}') \int d\mathbf{r}'' V_{tot}^{NL}(\mathbf{r},\mathbf{r}'')\varphi_k(\mathbf{r}'') = \delta(\mathbf{r}-\mathbf{r}'). \quad (38)$$

Recalling that the $\varphi_k(\mathbf{r})$ are solutions of the eigenvalue problem of equation (9), equation (38) becomes:

$$\sum_k A_k(\mathbf{r}')(\varepsilon_k-\varepsilon)\varphi_k(\mathbf{r}) = \delta(\mathbf{r}-\mathbf{r}'). \quad (39)$$

Multiplying both sides of equation (39) by $\varphi_j^*(\mathbf{r})$ and integrating over $\mathbf{r}$ one finally obtains:

$$A_j(\mathbf{r}') = \frac{\varphi_j^*(\mathbf{r}')}{\varepsilon_j-\varepsilon}. \quad (40)$$

Therefore, as in the local case [15], it is possible to write the Green's function as:

$$G(\mathbf{r},\mathbf{r}';\varepsilon) = \sum_j \frac{\varphi_j^*(\mathbf{r}')\varphi_j(\mathbf{r})}{\varepsilon_j-\varepsilon}. \quad (41)$$

Upon inserting equation (41) in equation (33) we get:

$$\chi^0(\mathbf{r},\mathbf{r}';\omega) = \sum_{i_{occ}} \varphi_i(\mathbf{r})\varphi_i^*(\mathbf{r}')G(\mathbf{r},\mathbf{r}';\varepsilon_i+\omega) + \sum_{i_{occ}} \varphi_i^*(\mathbf{r})\varphi_i(\mathbf{r}')G^*(\mathbf{r},\mathbf{r}';\varepsilon_i-\omega). \quad (42)$$

It is worth recalling that, due to the spherical symmetry of the problem, equations (31, 33, 34) are all diagonal with respect to the angular momentum components, and so they reduce to one-dimensional radial equations, one for each l.

In our calculation the Green's function is computed by discretizing the corresponding radial equation on a linear mesh, thus transforming it into a matrix equation. This is then inverted by adding a small imaginary part (γ) to the energy parameter in order to avoid the singularities at the (real) single-particle eigenvalues. For typical calculations we have used a mesh of 250 points extending from the center of the cluster out to three times the cluster's radius, whereas a value of 50 meV for the γ parameter has been used.

From the density-density correlation function all the dynamical quantities may be computed in the usual manner [15].

To assess the accuracy of our TDLDA numerical procedure we have compared the integrated photoabsorption cross-section $\sigma(\omega)$ with the optical $f-$sum rule modified to account for non-locality:

$$\int_0^\infty d\omega\sigma(\omega) = C(N + \Delta N) \tag{43}$$

where $C = (2\pi^2/c)$ a.u. and with $\Delta N = 0$ in the local case and

$$\Delta N = \frac{2}{3}\int_0^\infty dr \int_0^\infty dr' \sum_{nl}(2l+1)u_{nl}(r)u_{nl}(r') \times \sum_{l'}\left[2rr'(2l'+1)\begin{pmatrix} l & 1 & l' \\ 0 & 0 & 0 \end{pmatrix}^2 - \delta_{l',l}(r^2 + r'^2)\right] \times \Gamma_{l'}(r,r') \tag{44}$$

in the non-local one. In the present work, calculated TDLDA cross-sections fulfill the $f-$sum rule typically to better than 1 part in 10^3. Such value that we consider accurate enough can be further improved by reducing the mesh spacing (which affects the matrix inversion procedure to calculate the Green's function) at the cost, of course, of an increased computational overload.

3 Results and discussion

We have applied the above formalism to the calculation of the dipolar optical response of alkali metals, which constitute a typical benchmark to test the reliability of such calculations. We have focused our study on either Na or Li clusters in order to elucidate the inherent contribution of the non-locality, which is known to play a minor role in Na [3,8,16], whereas it is more relevant in the Li case [3,11,12,16–18]. The size of the clusters has been chosen to investigate to what extent one can push the approximation of radial averaging: for large clusters, in fact, this approximation works fairly well [12], as we will show below for Na_{138} and Li_{138}, but in the case of clusters made of a few atoms, it is well known that deviations from "sphericity" are relevant [5,19,20], so the applicability of any kind of spherical average (uniform or radial) of the electron-ion interaction is still under debate. Therefore, we focused our attention on clusters made up of 8 (closed-shell structures) and 6 (open-shell) atoms, for which reliable *ab initio* calculations [6,19–26] and experimental photoabsorption cross-section are available [22,23,27–30].

3.1 Na_2, Li_2

As a preliminary test, we have calculated the ground-state properties of the Na_2 and Li_2 dimers: the equilibrium distance d, the vibrational wave-number ν and the dissociation energy D_e are reported in Table 1 together with the experimental results of references [31,32] and the *ab initio* calculations of references [5,33].

Although the SAPS approximation is expected to be reliable mostly for spherically symmetric systems, we see that for both Na and Li a good agreement has been found between all the spectroscopic quantities considered and the corresponding experimental results; in the case of the vibrational frequency ν, NL-SAPS results are overestimated by 8% for Na and underestimated by 3% for Li, respectively: in any case, a perfect agreement with fully 3D *ab initio* results of references [5,33] is obtained, therefore assessing the reliability of our method. We note that in reference [13] for Li_2 the calculated dissociation energy is $D_e = 0.22$ eV which is well below the experimental value of $D_e^{exp} = 1.06$ eV (even if the calculated equilibrium distance is in good agreement with the experimental result). This suggests that complete inclusion of the p-nonlocality as in our approach instead of the single s-nonlocality used in references [12,13] is of relevant importance. Moreover, these results clearly demonstrate that the SAPS approximation, when combined with the non-local approach, is less severe than one could think. We now further investigate the reliability of our NL-SAPS in the case of closed- and open-shell alkali clusters.

3.2 Na_8

The starting points of all our calculations are the structures obtained with *ab initio* geometry optimizations of CI and MD type [19,20,24]. We did not repeat full structural optimization: we kept the symmetry of the ionic arrangement, while allowing the overall structure to expand or shrink with respect to the center of mass of the cluster by scaling the coordinates and finding a minimum of the total energy in this restricted configuration space. This ends up in a redefinition of the cluster volume, which in turns implies a different delocalization volume for the valence electrons with respect to either the simple jellium (JM) or the uniform averaged pseudo-jellium (UAPS) models.

Of course closed-shell structures are expected to be quite nicely represented by calculations involving spherically symmetric averages of the ionic potentials. Therefore our first aim is to compare the uniform average of reference [3] with our radial average in Na_8, in order to better elucidate the effect of the ionic structure.

We have adopted the T_d and D_{4d} space groups to represent the ground state geometries in the NL-SAPS calculations, while for the UAPS we have minimized the energy by varying the radius over which the uniform average had to be performed.

We stress the fact that our primary aim was the comparison between the two approximation schemes: the non-local uniform average of UAPS and our non-local version of the SAPS. Therefore we did not put emphasis on the systematic search of the absolute minimum in the total energy, so we have not taken into account other possible structures to represent the ground state geometry of the cluster (as, for example, the D_{2d} space group).

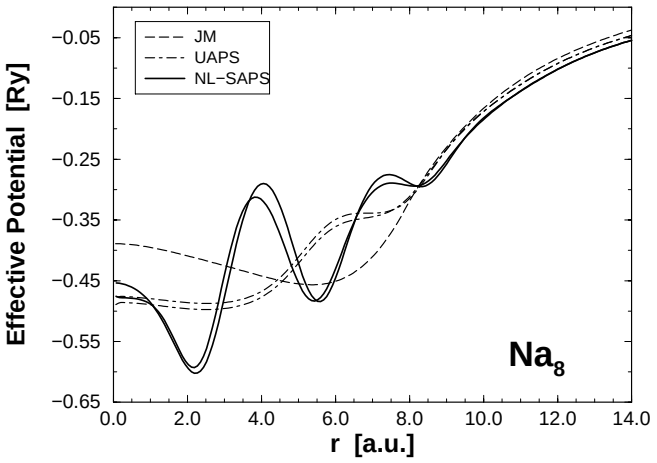

Fig. 1. Comparison among the self-consistent effective potentials for Na_8 in the T_d arrangement in jellium (JM), optimized UAPS and our NL-SAPS.

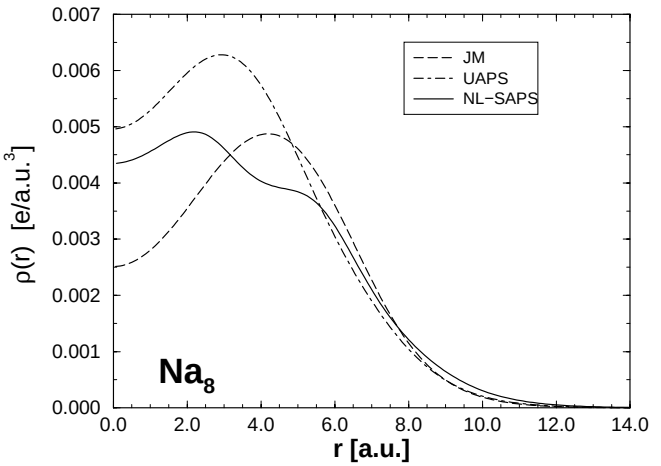

Fig. 2. Comparison among the electronic densities for Na_8 in the T_d arrangement in jellium (JM), optimized UAPS and our NL-SAPS.

It is worth noting that in its original formulation [3] the UAPS does not allow energy optimization because it *defines* the radius of the cluster in terms of the bulk Wigner radius. So in the following we compare our results also with this non-optimized version of UAPS (NO-UAPS). Another remark has to be done: in the case of UAPS, the calculation of the background ionic energy as the energy of a uniformly, positively charged sphere (as in JM) often leads to positive ground state energies (as in the case of Li clusters): so to better compare UAPS and NL-SAPS results also for the optimization of the UAPS structure we have used the discrete arrangements of T_d and D_{4d} space groups for the evaluation of the ionic potential energy.

With regard to the total energy minimization, there is a good agreement between our results and *ab initio* calculations: for the D_{4d} structure our minimum coincides with the one of CI calculations of reference [19], with a mean nearest-neighbor distance (MNND) of 0.345 nm which is lower than the bulk (b.c.c.) value 0.366 nm and also for the T_d case a MNND of 0.345 nm is found in agreement with MD and CI calculations. Nevertheless, at variance with CI calculations, our D_{4d} ground state geometry resulted to have lower total energy than the T_d one.

In Figure 1 we compare the effective potentials in the case of Jellium (JM), uniform average (UAPS) and our non-local SAPS for the T_d structure. The two curves for UAPS and NL-SAPS are the potentials which act on the $1s$ and $1p$ electrons and are obtained by building a "local" version [3] of the otherwise non-local potentials used in the Kohn-Sham equation, as follows:

$$V_{eff,nl}(r) = V_H(r) + V_{xc}(r) + \bar{V}^L_{SAPS}(r) + \frac{\int dr' \Gamma_l(r,r') u_{nl}(r')}{u_{nl}(r)}. \quad (45)$$

From this figure, one can see that while for Na non-local effects are not so pronounced for the UAPS case, the effective potentials being substantially independent on the orbital (see also Ref. [3]), in the NL-SAPS case the effects of the core electrons become more appreciable. It is also evident that in the case of UAPS, pseudo-potentials lead to a reduced binding of the valence electrons with respect to the JM and therefore to a larger electronic spill-out. This, in turns, affects the optical response by increasing the dipole polarizability. A more complex behavior has been obtained for the non-local SAPS. In this case, even if the tail of the potentials outside the cluster radius agrees with that of the UAPS (which is lower than the JM one), inside the cluster the potentials mimic the "two-shells" structure of the ionic arrangement in the T_d space group, visible in the two "peaks" near 4 a.u. and 7 a.u. Looking at the electronic densities (Fig. 2) one can see that non-local SAPS decreases a little bit the electronic binding with respect to UAPS and JM: this enhancement in the electronic spill-out outside the cluster radius implies as a by-product an increased polarizability in better agreement with experimental data. The result on the electronic density deserves some further comments: we can in fact test the reliability of our averaging procedure by comparing our data with those obtained with *ab initio* MD calculations by reference [20], in which a spherical average of the fully three-dimensional electronic density is reported. A good quantitative agreement between those results and ours NL-SAPS can be observed (and even more precise in the case of Na_6, as it will be shown below), which can not be obtained neither in the JM nor in the UAPS model, even in its non-local extension. This is a very important point because, as well known in DFT, it is the electronic density that triggers the whole physics of the system.

The TDLDA photoabsorption cross-section of Na_8 is plotted in Figure 3 for the T_d space group and compared with that of UAPS, with a lorentzian convolution of amplitude $\gamma = 0.05$ eV. A better agreement with experimental results of the position of the main resonance is found for the NL-SAPS, similarly to reference [16]. This spectrum also shows an increased Landau damping in the NL-SAPS, which redistributes part of the oscillator strengths to different single particle transitions.

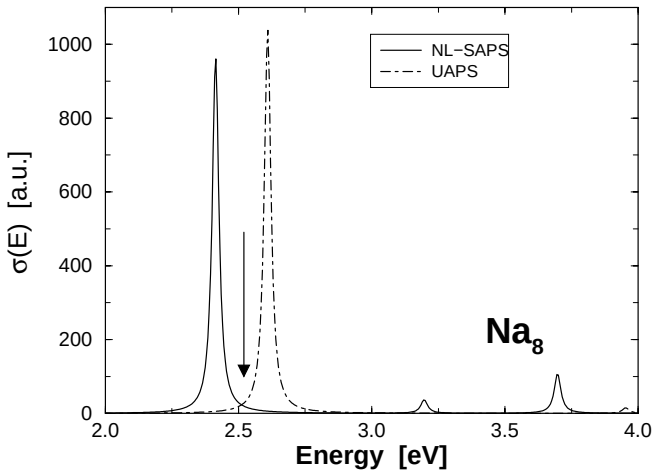

Fig. 3. Photoabsorption cross-section for Na_8 in the T_d arrangement in the optimized UAPS and our NL-SAPS. The vertical arrow is located at the main experimental resonance.

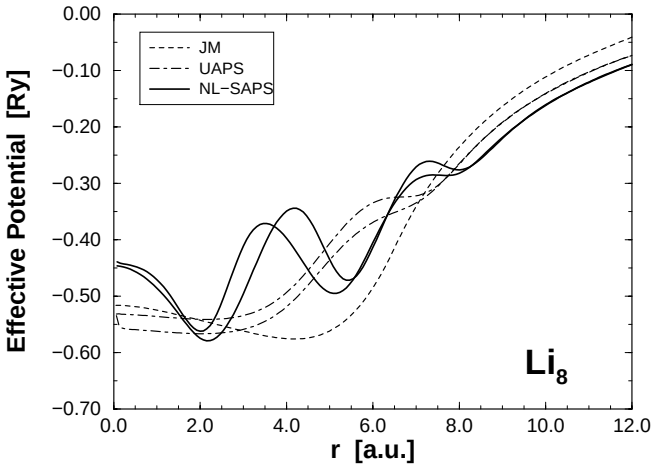

Fig. 4. Comparison among the self-consistent effective potentials for Li_8 in the T_d arrangement in jellium (JM), optimized UAPS and our NL-SAPS.

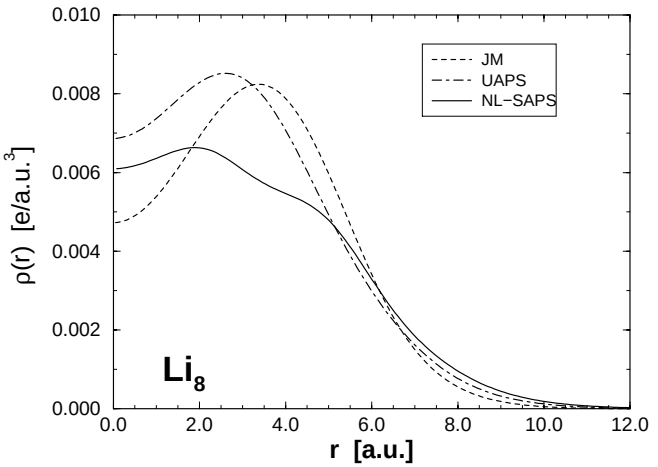

Fig. 5. Comparison among the electronic densities for Li_8 in the T_d arrangement in jellium (JM), optimized UAPS and our NL-SAPS.

The results of both static and dynamic calculations are summarized in Table 2, where the total energy, the cluster radius (defined with respect to the center of mass), the electronic spill-out, the RMS value of the electronic radius and the main peak in the photoresponse cross-section are reported for the T_d, the D_{4d} space groups for the NL-SAPS and UAPS case, respectively. Just for comparison also the analogous values in the non-optimized UAPS (NO-UAPS) and in the jellium (JM) case are included in the table, together with the experimental value of the optical response (OR) peak. From these data, as a first results, we conclude that the use of SAPS with realistic non-local pseudopotentials improves the quantitative agreement between theory and experiment with respect not only to the JM results, but also to the UAPS ones (optimized or not). It is worth noting that our calculation gives results which are very similar to the ones of reference [8], which included in a perturbative way the effect of the non-spherical part of the ionic potential, but using a semi-empirical (local) Heine-Abarenkov pseudo-potential. They obtained for instance a plasma resonance at 2.58 eV and 2.48 eV for the D_{4d} and T_d structure, respectively.

3.3 Li_8

A set of calculations similar to the ones for Na_8 have been carried out on Li_8. Also in this case we have minimized the total energy by rescaling two already optimized structures: the T_d structure resulting from CI calculations [24] and the structure obtained with *ab initio* MD [33] and LDA [25] calculations, which consists of a centered trigonal prism with an atom capping one of the rectangular faces ($CCTP$).

The energy minimum in our NL-SAPS calculations is obtained for the CCTP structure, with a MNND of 0.27 nm in very good agreement with the value of reference [25], whereas the T_d structure gives a MNND of 0.33 nm, which is larger than the CI one (0.31 nm) and the bulk (b.c.c.) one (0.302 nm).

The comparison of the effective potentials obtained for JM, UAPS and non-local SAPS is reported in Figure 4 for the T_d space group: the inherent non-local character of the potentials is now evident not only for the NL-SAPS but also for the UAPS case, and it is further enhanced with respect to the Na_8 case, emphasizing the importance of including non-locality in such systems. In Figure 5 the electronic densities are compared for the three cases examined. Also in this case there is a monotonic enhancement of the electronic spill-out and RMS electronic radius on going from JM, through UAPS, to NL-SAPS, which explains the increased red-shift of the NL-SAPS photoabsorption cross-section resonance (reported in Fig. 6) with respect to the other two cases, in better agreement with experimental data. With regard to the optical response calculations, we report the results in Table 3, whose entries are the same as in Table 2. An improvement with respect either to JM or UAPS is again obtained, even if *ab initio* calculations of reference [25] give of course better results than ours, predicting an energy of 2.45 eV for the

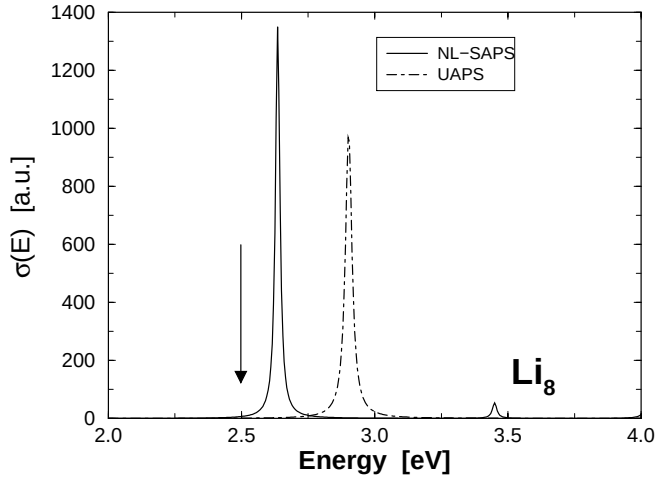

Fig. 6. Photoabsorption cross-section for Li_8 in the T_d arrangement in the optimized UAPS and our NL-SAPS. The vertical arrow is located at the main experimental resonance.

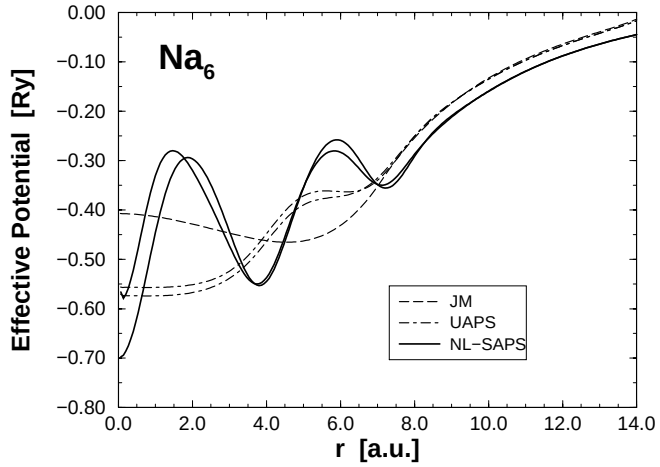

Fig. 7. Comparison among the self-consistent effective potentials for Na_6 in the C_{5v} arrangement in jellium (JM), optimized UAPS and our NL-SAPS.

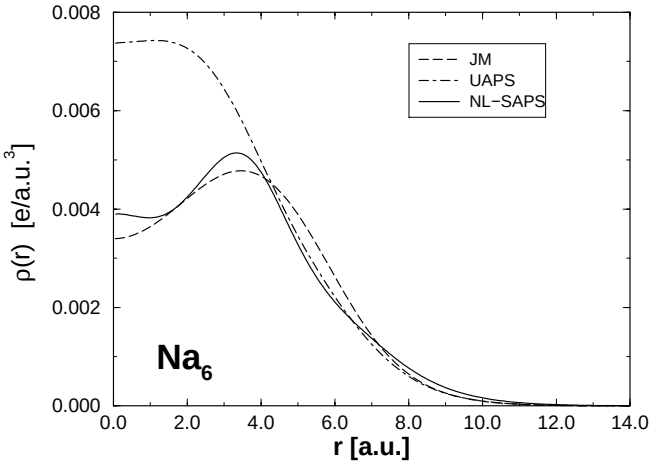

Fig. 8. Comparison among the electronic densities for Na_6 in the C_{5v} arrangement in jellium (JM), optimized UAPS and our NL-SAPS.

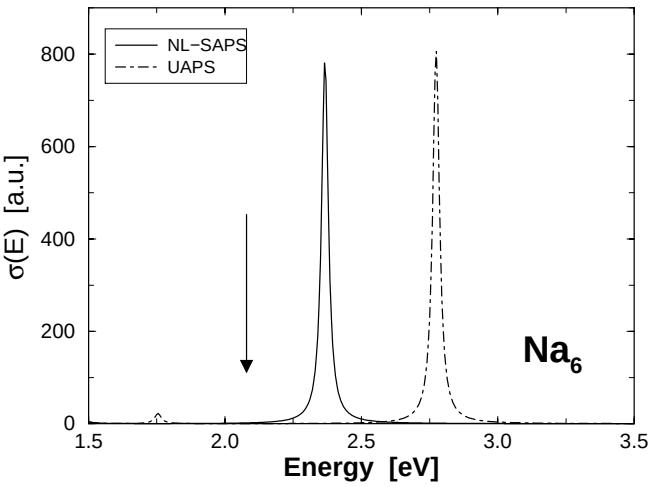

Fig. 9. Photoabsorption cross-section for Na_6 in the C_{5v} arrangement in the optimized UAPS and our NL-SAPS. The vertical arrow is located at the main experimental resonance.

Mie resonance, against an experimental results of 2.5 eV, therefore assessing the relevance of the precise ionic density.

3.4 Na_6

Since our scheme is found to produce a substantial improvement in the quantitative agreement between calculated and experimental results for the optical response of closed-shell systems, we have tested our approximation in the case of open-shell systems like the alkali hexamers, which up to now were not studied within the SAPS model.

The first open-shell structure investigated is Na_6 in the C_{5v} structure obtained by MD calculations of references [20,21]: Figure 7 gives a comparison of the self-consistent effective potentials for JM, UAPS and NL-SAPS.

The results on the electronic density are reported in Figure 8: it is worth noting the good quantitative agreement of our electronic density with the spherically averaged one of reference [20], obtained from *ab initio* MD calculations. All the relevant calculated static and dynamic properties are summarized in Table 4.

With regard to the photoabsorption cross-section of Figure 9, we note that while NL-SAPS is able to give a better quantitative agreement than both JM and UAPS in the position of the collective dipole resonance around 2.1 eV, it fails to reproduce the finer details of the experimental spectra [22]. A comparison with local pseudopotential calculation of reference [8] shows that the inclusion (at least perturbatively) of the non-spherical part of the background potential is mandatory in such structure to recover the experimental fine structures. The fact that our NL-SAPS formulation is not so satisfactory in "correcting" the local SAPS predictions, as compared to the Li case, corroborates the conclusion that non-local corrections in Na seems to play a minor role.

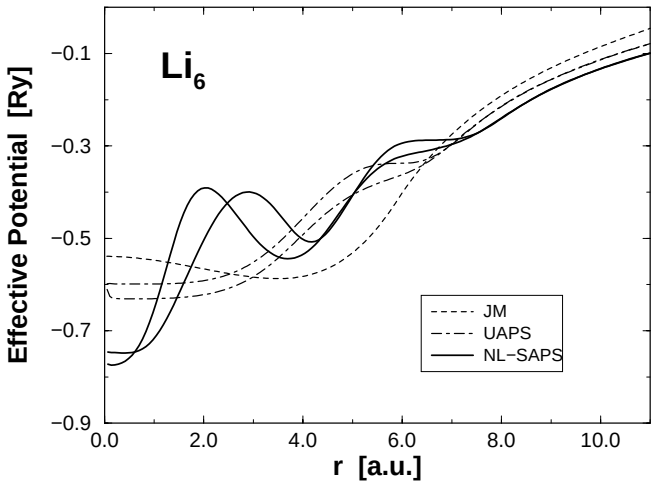

Fig. 10. Comparison among the self-consistent effective potentials for Li_6 in the C_{2v} arrangement in jellium (JM), optimized UAPS and our NL-SAPS.

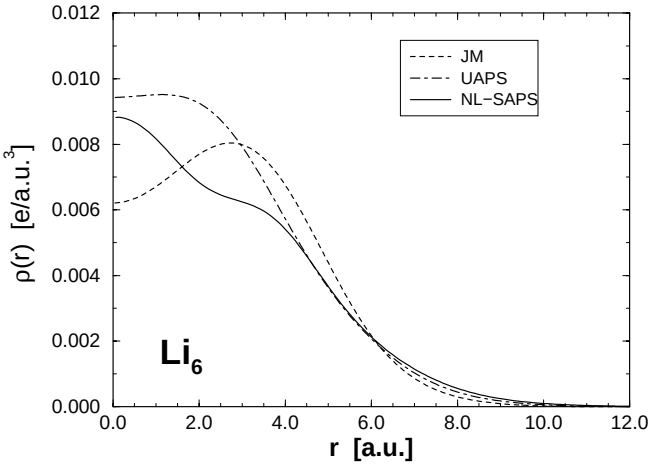

Fig. 11. Comparison among the electronic densities for Li_6 in the C_{2v} arrangement in jellium (JM), optimized UAPS and our NL-SAPS.

3.5 Li_6

For Li_6 we have compared two structures obtained by CI calculations [30]: the pentagonal pyramid (space group C_{5v}), which, due to its almost 2D character, shows a large deviation from spherical symmetry, and the nonplanar tripyramidal C_{2v} geometry, the last structure being "more three-dimensional" than the C_{5v} case.

In the energy minimization, we obtained for the C_{2v} structure (which has the lowest total energy, in agreement with Ref. [30]) an "expansion" of about 4% with respect to the CI result, whereas for the C_{5v} we got a contraction of about 5%. The effective potentials are reported for JM, UAPS and NL-SAPS in Figure 10 for the C_{2v} case. It is worth noting the remarkable non-locality in the NL-SAPS case. The electronic density of the NL-SAPS is compared in Figure 11 with those of JM and UAPS. As in the case of Li_8 there are not available averaged *ab initio* calculated density to check the reliability of our calculation.

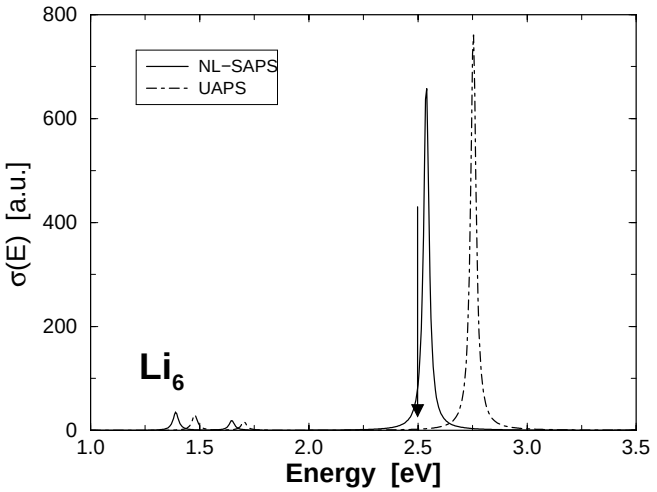

Fig. 12. Photoabsorption cross-section for Li_6 in the C_{2v} arrangement in the optimized UAPS and our NL-SAPS. The vertical arrow is located at the main experimental resonance.

The ground state data, together with the optical response peak are reported in Table 5.

Even if the deviation from sphericity is remarkable, also in this case we have a better quantitative agreement in the position of the main OR peak at 2.5 eV with respect to JM and UAPS, as it can be seen from Figure 12. Of course, the radial averaging procedure makes hard to grasp all the minor features in the experimental spectra (like the weak peak at 1.8 eV, which is only approximated by our calculated features around 1.5–1.6 eV): so we underline the fact that in our case we have not the possibility to discriminate between different isomers solely from the point of view of a simple optical response analysis, as can be done in the full *ab initio* CI calculation of references [24,30], who obtained for the C_{5v} structure a single intense peak located at 2.07 eV, therefore suggesting that the C_{2v} geometry (whose spectra agrees quantitatively in their calculations with the experimental one) is the most stable one.

3.6 Na_{138}, Li_{138}

In order to demonstrate the reliability of our method also with "large" systems, we have performed NL-SAPS calculations on clusters composed of 138 atoms arranged in the b.c.c. lattice sites as in the bulk. Structural minimization gives a 3% contraction for Na and an expansion of 8% for Li as compared to their respective bulk lattice parameters. The TDLDA optical response shows a main peak at 2.85 eV and 3.05 eV for Na_{138} and Li_{138}, respectively [34], which are in good agreement with the experimental values [35,36]. This supports our initial statement that the non-local SAPS scheme appears as a very effective tool for reliable calculations of the optical properties of large *and* small alkali clusters at a computer cost comparable to the simple jellium one, but with an enhanced degree of accuracy.

Table 1. Equilibrium distance d, vibrational wave-number ν and dissociation energy D_e of Na_2 and Li_2 calculated within NL-SAPS approach.

	Na_2			Li_2		
	NL-SAPS	*ab initio*(*)	exp.(**)	NL-SAPS	*ab initio*(†)	exp.(‡)
d (a.u.)	5.86	5.48	5.818	5.46	5.29	5.05
ν (cm^{-1})	171	173	159.1	341	341	351
D_e (eV)	0.75	0.91	0.747	0.96	1.03	1.06

(*) Ref. [5], (**) Ref. [31]; (†) Ref. [33], (‡) Ref. [32].

Table 2. Comparison between non-local spherical averaged pseudo-jellium (NL-SAPS), uniformly averaged pseudo-jellium (UAPS) and Jellium (JM) static and dynamic properties for Na_8.

Na_8	NL-SAPS		UAPS		NO-UAPS	JM	
	T_d	D_{4d}	T_d	D_{4d}			exp.(*)
E_{min} [Ry]	−3.336	−3.393	−3.767	−5.344	−0.169	−1.152	-
R_{min} [a.u.]	6.76	5.39	6.75	5.56	7.86	7.86	-
Spill-out	2.97	4.93	2.70	3.40	2.19	1.43	-
RMS radius [a.u.]	6.57	6.56	6.28	5.59	6.98	6.42	-
OR-peak [eV]	2.41	2.62	2.62	3.15	2.25	2.80	(2.52)

(*) Experimental result taken from [27].

Table 3. Comparison between non-local spherical averaged pseudo-jellium (NL-SAPS), uniformly averaged pseudo-jellium (UAPS) and Jellium (JM) static and dynamic properties for Li_8.

Li_8	NL-SAPS		UAPS		NO-UAPS	JM	
	T_d	CCTP	T_d	CCTP			exp.(*)
E_{min} [Ry]	−3.490	−3.607	−3.971	−4.398	0.305	−1.097	-
R_{min} [a.u.]	6.15	5.48	6.09	5.78	6.50	6.50	-
Spill-out	3.03	3.47	2.78	2.93	2.60	1.65	-
RMS radius [a.u.]	6.06	5.73	5.76	5.57	6.02	5.44	-
OR-peak [eV]	2.64	2.73	2.90	3.05	2.70	3.50	(2.50)

(*) Experimental result taken from [23].

Table 4. Comparison between non-local spherical averaged pseudo-jellium (NL-SAPS), uniformly averaged pseudo-jellium (UAPS) and Jellium (JM) static and dynamic properties for Na_6.

Na_6	NL-SAPS	UAPS	NO-UAPS	JM	
	C_{5v}	C_{5v}			exp.(*)
E_{min} [Ry]	−2.291	−3.021	−0.071	−0.771	-
R_{min} [a.u.]	5.56	5.75	7.14	7.14	-
Spill-out	3.11	2.50	1.88	1.29	-
RMS radius [a.u.]	6.30	5.78	6.58	5.96	-
OR-peak [eV]	2.36	2.78	2.22	2.70	(2.08)

(*) Experimental result taken from [22].

Table 5. Comparison between non-local spherical averaged pseudo-jellium (NL-SAPS), uniformly averaged pseudo-jellium (UAPS) and Jellium (JM) static and dynamic properties for Li_6.

Li_6	NL-SAPS		UAPS		NO-UAPS	JM	
	C_{2v}	C_{5v}	C_{2v}	C_{5v}			exp.(*)
E_{min} [Ry]	−2.496	−2.377	−2.623	−3.078	0.286	−0.699	-
R_{min} [a.u.]	5.80	5.05	5.83	5.31	5.90	5.90	-
Spill-out	2.29	2.97	2.25	2.46	2.22	1.47	-
RMS radius [a.u.]	5.77	5.69	5.67	5.35	5.72	5.07	-
OR-peak [eV]	2.54	2.62	2.75	3.02	2.72	3.35	(2.50)

(*) Experimental result taken from [30].

4 Conclusions

In this paper we have presented analytic calculation to include in a complete way the non-local contribution to the electron-ion interaction arising from norm-conserving pseudo-potentials in the spherical averaged jellium model (SAPS). We have applied this model to the calculation of the dipole optical response of alkali metals hexamers and octamers and we have compared our approach with the uniform average jellium model (UAPS) in order to elucidate the relevance of the ionic structure. Our results show that an increased reliability of the SAPS approximation can be achieved when norm-conserving *ab initio* pseudopotentials are used, due to the non-local effect of the core electrons, which results in a better quantitative agreement with experimental data. With respect to the simple uniform averaged UAPS model we have obtained systematic improvements when the "ionic granularity" is taken into account even in the approximate way implied by the SAPS scheme. Indeed, even for remarkably non-spherical, open-shell systems, our formalism is able to give reasonably good quantitative results: nevertheless in order to obtain a greater accuracy also in the reproduction of the minor features of the optical response a more precise account for the actual ionic distribution (at least in a perturbative way) is advisable. In conclusion the non-local SAPS model also due to its modest computer cost (slightly higher than the simple jellium one) demonstrated to be a viable route to the calculation of static and dynamic properties of clusters in a large size range bridging the gap between *ab initio* and jellium-type calculations.

References

1. M. Brack, Rev. Mod. Phys. **65**, 677 (1993).
2. W. Ekardt, Phys. Rev. B **29**, 1558 (1984).
3. F. Alasia, Ll. Serra, R.A. Broglia, N. Van Giai, E. Lipparini, H.E. Roman, Phys. Rev. B **52**, 8488 (1995).
4. G.B. Bachelet, D.R. Hamann, M. Schlüter, Phys. Rev. B **26**, 4199 (1982).
5. J.L. Martins, J. Buttet, R. Car, Phys. Rev. B **31**, 1804 (1985).
6. I. Moullet, J.L. Martins, F. Reuse, J. Buttet, Phys. Rev. Lett. **65**, 476 (1990).
7. M.P. Iñiguez, M.J. Lopez, J.A. Alonso, J.M. Soler, Z. Phys. D **11**, 163 (1989).
8. W.D. Schöne, W. Ekardt, J.M. Pacheco, Phys. Rev. B **50**, 11079 (1994).
9. A. Rubio, L.C. Balbas, J.A. Alonso, Phys. Rev. B **45**, 13657 (1992).
10. W.D. Schöne, W. Ekardt, J.M. Pacheco, Z. Phys. D **36**, 65 (1996).
11. S.A. Blundell, C. Guet, Z. Phys. D **28**, 81 (1993).
12. S.A. Blundell, C. Guet, Z. Phys. D **33**, 153 (1995).
13. A. Bol, M.J. Stott, J.A. Alonso, Physica B **240**, 154 (1997).
14. J.P. Perdew, A. Zunger, Phys. Rev. B **23**, 5048 (1981).
15. A. Zangwill, P. Soven, Phys. Rev. B **21**, 1561 (1980).
16. J.M. Pacheco, J.L. Martins, J. Chem. Phys. **106**, 6039 (1997).
17. Ll. Serra, G.B. Bachelet, N. Van Giai, A. Lipparini, Phys. Rev. B **48**, 14708 (1993).
18. P. Alippi, P. La Rocca, G.B. Bachelet, Phys. Rev. B **55**, 13835 (1997).
19. V. Bonacic-Koutecky, P. Fantucci, J. Koutecky, J. Chem. Phys. **93**, 3802 (1990).
20. U. Röthlisberger, W. Andreoni, J. Chem. Phys. **94**, 8129 (1991).
21. V. Bonacic-Koutecky, J. Pittner, C. Scheuch, M.F. Guest, J. Koutecky, J. Chem. Phys. **96**, 7938 (1992).
22. C.R.C. Wang, S. Pollack, T.A. Dahlseid, G.M. Koretsky, M.M. Kappes, J. Chem. Phys. **96**, 7931 (1992).
23. J. Blanc, V. Bonacic-Koutecky, M. Broyer, J. Chevaleyre, Ph. Dugourd, J. Koutecky, C. Scheuch, J.P. Wolf, L. Wöste, J. Chem. Phys. **96**, 1793 (1992).
24. I. Boustani, W. Pewestorf, P. Fantucci, V. Bonacic-Koutecky, J. Koutecky, Phys. Rev. B **35**, 9437 (1987).
25. A. Rubio, J.A. Alonso, X. Blase, L.C. Balbas, S.G. Louie, Phys. Rev. Lett. **77**, 247 (1996).
26. R. Rousseau, D. Marx, Phys. Rev. Lett. **80**, 2574 (1998).
27. C.R.C. Wang, S. Pollack, D. Cameron, M.M. Kappes, J. Chem. Phys. **93**, 3787 (1990).
28. K. Selby, V. Kresin, J. Masui, M. Vollmer, W.A. de Heer, A. Scheidemann, W.D. Knight, Phys. Rev. B **43**, 4565 (1991).
29. W.A. de Heer, Rev. Mod. Phys. **65**, 611 (1993).
30. Ph. Dugourd, J. Blanc, V. Bonacic-Koutecky, J. Chevaleyre, M. Broyer, J. Koutecky, J. Pittner, J.P. Wolf, L. Wöste, Phys. Rev. Lett. **67**, 2638 (1991).
31. K.K. Verma, J.T. Bahns, A.R. Rejei-Rizi, W.C. Stwalley, W.T. Zemke, J. Chem. Phys. **78**, 3599 (1983).
32. R. Kawai, J.F. Tombrello, J.H. Weare, Phys. Rev. A **49**, 4236 (1994).
33. M.W. Sung, R. Kawai, J.H. Weare, Phys. Rev. Lett. **73**, 3552 (1994).
34. G. Mattei, F. Toigo, to be published.
35. P. Meibom, M. Østergård, J. Borggreen, S. Bjørnholm, H.D. Rasmussen, Z. Phys. D **40**, 258 (1997).
36. C. Bréchignac, Ph. Cahuzac, J. Leygnier, A. Sarfati, Phys. Rev. Lett. **70**, 2036 (1993).